ISSN 1068-3739, Russian Meteorology and Hydrology, 2021, Vol. 46, No. 8, pp. 495–506. Allerton Press, Inc., 2021.
Russian Text The Author(s), 2021, published in Meteorologiya i Gidrologiya, 2021, No. 8, pp. 5–20.

Parameterization of Shortwave Solar Radiation in Glaciological Applications

O. O. Rybak[a, b, c]*, R. Satylkanov[d, e], E. A. Rybak[b, c], A. S. Gubanov[f], I. A. Korneva[c, g], and K. Tanaka[h]

[a]*Water Problems Institute, Russian Academy of Sciences, ul. Gubkina 3, Moscow, 119333 Russia*
[b]*Subtropical Scientific Center, Russian Academy of Sciences, ul. Ya. Fabriziusa 2/28, Sochi, 354002 Russia*
[c]*Branch of Institute of Natural and Technical Systems, Kurortnyi pr. 99/18, Sochi, 354002 Russia*
[d]*Tien Shan High Mountains Scientific Center at the Institute of Water Problems and Hydropower of the National Academy of Sciences of Kyrgyz Republic, ul. Pionerskaya 9, Kyzyl Suu, 722000 Kyrgyzstan*
[e]*Scientific Research Center of Ecology and Environment of the Central Asia, Erkindik blvd, Bishkek, 720040 Kyrgyzstan*
[f]*Lomonosov Moscow State University, GSP-1, Leninskie Gory, Moscow, 119991 Russia*
[g]*Institute of Geography, Russian Academy of Sciences, Staromonetny per. 29, Moscow, 119017 Russia*
[h]*University of Kyoto, Yoshida-honmachi, Sakyo-ku, Kyoto, 606-8501 Japan*
**e-mail: o.o.rybak@gmail.com*

Received October 9, 2020
Revised January 16, 2021
Accepted April 6, 2021

Abstract—Solar irradiance is the most important factor which determines the thermal conditions of mountain glaciers. We use trigonometric formulae to calculate direct solar radiation incoming on any arbitrary oriented surface under the condition of absence of the atmosphere. Shading effect from the surrounding relief can also be evaluated rather precisely. Nevertheless, in order to obtain correct results, it is necessary to take into account atmospheric transmissivity, diffuse radiation, and influence of cloudiness. The paper presents a model for calculation of shortwave radiation, utilizing up-to-date data on the atmospheric composition and schemes for parameterization of the atmospheric transmissivity, which have never been implemented in glaciological applications before. Validation of the model was carried out using observational data on the global radiation on two weather stations established on Karabatkak glacier (Inner Tien Shan).

DOI: 10.3103/S106837392108001X

Keywords: Solar radiation, shortwave radiation, thermal conditions of mountain glaciers, surface mass balance of glaciers, parameterization of radiational processes

1. INTRODUCTION

Water resources of mountain and piedmont territories are dependent on glacial meltwaters, especially in arid regions. For instance, in the internal regions of the Tien Shan the annual amount of precipitation equals 300–400 mm/year. Therefore, glaciers contribute crucially to river runoff [3]. Prediction of available water resources, especially in long perspective under climatic change, is impossible without reliable estimates of mountain glaciers dynamics using application of appropriate mathematical models. The starting point in elaboration of a mathematical model of dynamics of a mountain glacier is calculation of surface mass balance. The discharge part of the balance, surface melting, is determined by the amount of available energy. In contrast to income part of the balance, accumulation, ablation can be well formalized from the basic physical principles. Intensity of the main source of energy required for surface melting, shortwave radiation [8], can be calculated basing on well-known trigonometric expressions, which determine the Sun position

in the sky and orientation in space of a section of the mountain glacier, as well as by taking into account attenuating factors: molecular scattering, absorption by water vapor and aerosols, etc. To calculate the latter (for calculation, in fact, the transmissivity of the atmosphere), mathematical models of varying degrees of complexity are used. Parametrization of radiation processes is facilitated by two circumstances: the increase in the total amount and availability of data on the state of the atmosphere and the possibilities for the calibration and validation of radiation models on the data of automatic weather stations established directly on the mountain glaciers.

In the radiation models that are used as components of modern surface mass balance models or, more broadly, dynamic models of mountain glaciers, simplified approaches to parameterize the transmissivity of the atmosphere and to estimate the ratio of direct and diffuse radiation are mainly implemented [4, 6, 7, 16]. At the same time, dozens of radiation models exist allowing more accurate calculation of radiation fluxes compared to approaches used in traditional glaciological models, and, more importantly, prompt implementation of the latest data on changes in the composition of the atmosphere [11, 13, 14]. Applying these models could significantly increase the accuracy of predictions of the state of mountain glaciation, its sensitivity to variations in the composition of the atmosphere, because the corresponding changes can be directly embedded into the model. The aim of this study was to revise critically some of the key algorithms for calculating radiation fluxes in glaciological models and to improve their reliability.

All mathematical surface mass balance models based on the energy balance approach [5, 6, 16, 18] (the alternative approach is the temperature index method [20]), require calculation of the net radiation on the surface of a glacier. For this purpose, one needs to estimate the global (direct and diffuse) radiation incoming on the arbitrary oriented glacial surface, longwave incoming and outgoing radiation, to consider influence of cloudiness, shading effect from the surrounding relief, changes in surface albedo, presence of debris cover etc. Global radiation makes maximum contribution in formation of conditions favorable to surface melting of a glacier. At the same time, it can be most realistically formulated in terms of a mathematical model (in contrast to, for instance, the turbulent heat exchange of a glacier with the atmospheric or internal and avalanche feeding). The following main factors determine the most significant changes of direct and diffuse radiation fluxes: the height of the Sun (or, equivalently, the mass of the atmosphere in the direction of the Sun), transmissivity of the atmosphere, cloudiness, duration of sunshine [1].

In the paper, we consider the radiation model adapted for the mountain glacier and present results of simulation of direct and diffuse radiation on Karabatkak glacier (northern macro-slope of the Terskey Ala-Too mountain ridge, Inner Tien Shan). The choice of this particular glacier is explained by the fact that observations of the surface mass balance components have been conducted here during several decades. Observations were interrupted for several years at the end of the 20th–beginning of the 21st centuries (as on most of the glaciers of the former USSR). Model prognostic calculations of the mountain glaciation evolution in the Tien Shan require preliminary model calibration and validation, therefore, it is important to use historical observation records. Another reason for choosing Karabatkak is that two automatic weather stations (AWS) are installed in the ablation zone of the glacier (Fig. 1). Data from these AWS were very helpful for model tuning.

The study consists of two parts. In the first part (this paper) we consider the issues of shortwave simulation. In the second part we shall study simulation of the longwave radiation and net radiation (radiation balance).

2. ALGORYTHMS OF THE GLOBAL RADIATION CALCULATION

Following the works [13, 14], we can formulate global radiation E_S at the surface of the Earth and under condition of absence of the cloud cover as the sum

$$E_S \quad E_{dir} \quad E_{dif} \quad \widetilde{E}_{dif} \tag{1}$$

where E_{dir} is direct radiation; E_{dif} is diffuse radiation; $\widetilde{E}_{dif}$ is multiple reflected diffuse radiation.

Trigonometric expressions linking the position of the Sun and irradiance on the top of the atmosphere and at the surface of the Earth are described in detail, for instance, in the classical monograph [12]. Therefore, listed below are only key expressions, which are necessary for understanding computational algorithms.

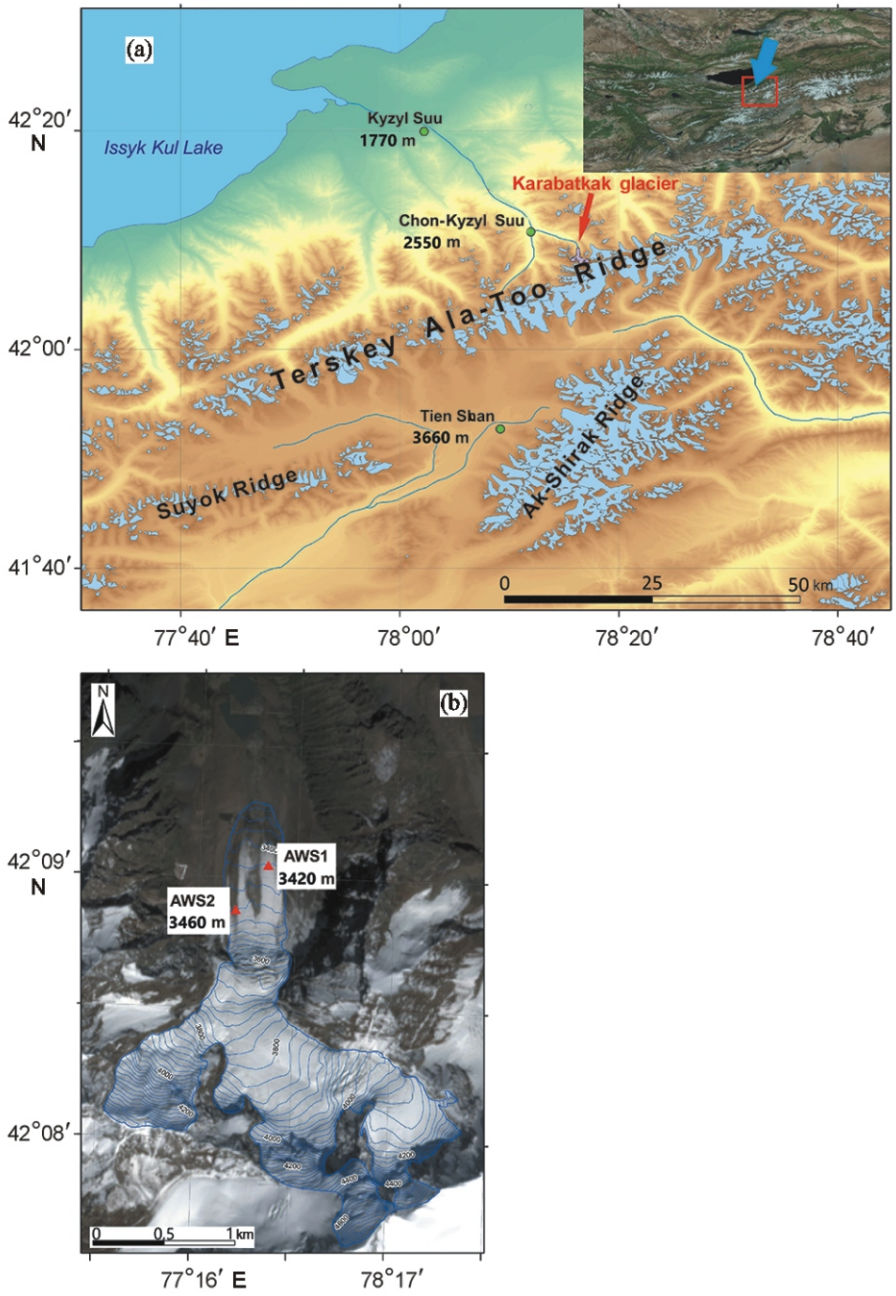

Fig. 1. The region of the research is Inner Tien Shan: (a) Karabatkak glacier is located on the northern slope of the Terskey Ala-Too mountain ridge; outlined in the inset by the red frame, is the region of the research; the arrow indicates the location of the AERONET Issyk Kul station; the satellite image of Karabatkak glacier (b; isolines are drawn every 20 m); the red triangles indicate locations of the automatic weather stations AWS1 and AWS2.

2.1. Direct Radiation

According to the model of Iqbal [12], which, in turn, is based on the series of earlier studies, direct solar radiation E_{dir}, incoming on the horizontal plane in the absence of clouds can be estimated as

$$E_{\text{dir}} \quad SR_0(\cos\ )t_R\, t_g\, t_n\, t_w\, t_a\, t_o \tag{2}$$

where S is the solar constant; R_0 is correcting coefficient accounting for ellipticity of the Earth's orbit:

$$R_0 \quad 1.00010 \quad 0.034221\cos \quad 0.001280\sin \quad 0.000719\cos 2 \quad 0.000077\sin 2 \tag{3}$$

Table 1. Mean annual data on the atmospheric parameters and corresponding mean square errors at the Issyk Kul station

Parameter	January	February	March	April	May	June	July	August	September	October	November	December
$_{500}$	0.116	0.119	0.157	0.228	0.113	0.114	0.137	0.141	0.136	0.105	0.091	0.088
	0.059	0.073	0.105	0.241	0.068	0.064	0.073	0.088	0.077	0.065	0.056	0.048
	1.48	1.31	0.94	0.80	1.10	1.28	1.43	1.27	1.21	1.22	1.41	1.56
	0.032	0.036	0.046	0.048	0.035	0.041	0.036	0.035	0.040	0.042	0.037	0.031
	0.042	0.048	0.082	0.131	0.053	0.047	0.051	0.058	0.059	0.045	0.034	0.030
	0.130	0.127	0.239	0.267	0.304	0.351	0.375	0.400	0.375	0.314	0.145	0.127
	0.437	0.428	0.390	0.384	0.384	0.327	0.183	0.152	0.259	0.346	0.339	0.437
w	0.41	0.39	0.53	0.70	0.99	1.26	1.42	1.33	1.07	0.83	0.59	0.42
$_{w}$	0.16	0.16	0.16	0.20	0.26	0.28	0.23	0.31	0.24	0.25	0.20	0.16

Explanations are given in the text.

where 2 (d_n 1)/365 is day angle in radians; d_n is the day of the year. Other coefficients in (2) are responsible for attenuating of the solar radiation in the atmosphere: as a result of Rayleigh scattering (t_R), scattering and absorbtion by aerosols (t_a), ozone (t_o), nitrogen dioxide (t_n), uniformly mixed gases (t_g), water vapor (t_w); is the solar zenith angle:

$$\arccos(\sin \sin \cos \cos \cos) \quad (4)$$

where is geographical latitude; is declination of the Sun; is hour angle of the Sun. Comparison of several methods of parameterization of direct shortwave radiation showed that the Iqbal model, despite the fact that it was proposed more than 30 years ago, is very effective in terms of ability to reproduce the actual values of shortwave radiation at the Earth's surface [19]. The efficiency of the Iqbal model is determined apparently by parameterization of attenuating coefficients in (2).

Note that the method of Iqbal (so called model C [11]) of calculation of transmissivity of the atmosphere is implemented in other models, but using other parameterizing equations for the coefficients t_R, t_a, t_o, t_n, t_g, and t_w. The Iqbal model sets a kind of scheme for calculating transmissivity, and individual coefficients are determined based on the analysis of an increasing array of observational data. In our study, these coefficients are calculated in accordance with the REST model (Reference Evaluation of Solar Transmittance) [11]. The form of parameterizing equations in the REST model allows using the optimum way to assimilate the data of observations of the atmosphere composition, which were not fully available in the beginning of 1980s. Used as input variables in the REST model (see Table 1 in [11]), are the atmospheric pressure *p*, contents of water vapor *w*, ozone u_o and nitrogen dioxide u_n in the unit atmospheric column, extinction coefficient and zenith angle of the Sun (4).

The extinction coefficient is derived from the Angstrom law:

$$( ) \quad (5)$$

where ( ) is aerosol optical depth on the wavelength ; is Angstrom exponent. Aerosol optical depth ( ) on the wavelength 500 nm ($_{500}$) is most often used to characterize aerosol attenuation of radiation in the atmosphere. Mean monthly values of $_{500}$ and and their mean square errors for the range 440–870 nm were calculated for the period 2007–2016 at Issyk Kul station (42 37 N, 76 58 E, 1650 m above sea level). The station is located relatively close to Karabatkak glacier (Fig. 1). The data are free available at the site of Aerosol Robotic Network (AERONET, https://aeronet.gsfc.nasa.gov). Data on the atmospheric water vapor content *w* are also available there (Table 1). The extinction coefficient apparently varies during the year in broad limits, remaining, however, relatively low due to the low content of impurities. Shown for comparison in lines and , are values for stations Dakka (Bangladesh) and Dushanbe (Tajikistan), which are on average an order of magnitude higher than on Issyk Kul station. Since the Dushanbe station is located in natural conditions similar to Issyk Kul station, the reasons for the higher values of the extinction coefficients can be entirely attributed to the anthropogenic impact.

Mean monthly values of ozone content (in Dobson units) during the period of 1997–2005 in the latitudinal belt 40 –45 N were taken from [9]. Nitrogen dioxide concentration in the troposphere depends to the great extent from the degree of anthropogenic pollution. In accordance to [11], we assume the constant value in the unit atmospheric column (both troposphere and stratosphere) $u_n = 1.5$ 10^{-4} atm-cm, which is

typical for the clean atmosphere. Mean monthly values of the atmospheric pressure (necessary for calculation of the Rayleigh scattering) are taken from observations on the AWS.

The surface of the glacier is arbitrary oriented in space. This circumstance should be taken into account for calculation of direct radiation, therefore, instead of the zenith angle in (3) it is necessary to use angle between the normal to the plane and direction to the Sun [2].

2.2. Diffuse Radiation

For purpose of mathematical modeling, in the majority of cases, diffuse radiation is considered isotropic, though in reality its greater part falls from the cloudless sky from the direction of the Sun. An isotropic model, strictly speaking, is fully consistent only in overcast conditions [2]. Nevertheless, an isotropic model is employed because of the lack of observations. In this study, diffuse radiation under the condition of absence of clouds is calculated in accordance with the approach formulated in the model MRM, version 6.1 [13], taking into account sky view factor f_s and reflection from the surrounding relief E_t [7]:

$$E_{dif} \quad f_s SR_0(\cos \quad)t_g t_n t_w t_{aa}(0.5f_a)^{0.5}(1 \quad t_{as}t_R) \quad E_t \tag{6}$$

where $t_{aa} = t_a/t_{as}$ is the attenuation of the solar radiation due to absorption by aerosols; t_{as} is attenuation due scattering by aerosols (Mie scattering):

$$t_{as} \quad \exp(\ m_R SSA\ ). \tag{7}$$

In (7) *SSA* is single-scattering albedo; $_{500}$ is monthly mean of aerosol optical depth at the Issyk Kul station (Table 1); m_R is mass of the atmosphere, parametrized in accordance with [11]:

$$m_R \quad (p/1013.25)[\cos \quad 0.48353 \ ^{0.095846}/(96.741 \quad)^{1.754}]\ ^{1}. \tag{8}$$

The term $(0.5f_a)^{0.5}$ defines the shares of the Rayleigh and aerosol scatterings, which reach surface of the Earth. In the ideal case this term equals to 0.5, though in reality the flux of diffuse radiation in the direction of the surface of the Earth is greater compared to the flux in the opposite direction and depends solely on the solar altitude $= 90 - :$

$$f_a \quad 8 \quad 10^{5\ 2} \quad 0.0117 \quad 0.5. \tag{9}$$

In this study, the tuned parameter *SSA* varies within the limits 0.65–1.0 [15]. Reflection from the surrounding relief E_t is calculated in accordance with [7]:

$$E_t \quad _t(1 \quad f_s)E_S \tag{10}$$

where $_t$ is the surface albedo. Apparently, to estimate E_t it is necessary to calculate E_S without this term and next to make appropriate correction.

Radiation in a cloudless sky due to a single reflection from the Earth's surface and subsequent molecular (Rayleigh) and aerosol scattering, $\widetilde{E}_{dif}$, is small compared with E_{dif} [14]. Nevertheless, to accurately calculate incoming radiation, especially over fresh snow with high albedo, it is reasonable to take into account this component:

$$\widetilde{E}_{dif} \quad (E_{dir} \quad E_{dif})[\ _g\ _s/(1 \quad _g\ _s)] \tag{11}$$

where $_s$ is the cloudless sky albedo; $_g$ is surface albedo. In the current study, $_g = 0.8$ for the snow-covered surface, $_g = 0.3$ for clear ice; $_s \quad _R \quad _a$; $_R = 0.0685$ is the albedo of Rayleigh scattering, $_a = 0.16(1 - t_a)$ is the albedo of scattering by aerosols [14].

2.3. Impact of Clouds

Probably, the most difficult term for parameterization in surface mass balance modeling and, at the same time, the most uncertain is the cloud factor [8, 21]. Clouds influence radiation fluxes in different ways. Depending on the type of clouds and the height of the Sun, a cloud layer can either be almost transparent for the direct solar radiation, or block radiation completely [1]. On the one hand, observations of cloudiness (types of clouds, cloud amount) are carried out at meteorological stations closest to the glacier, and their results can be used to calculate past or current values of the surface mass balance. Note that quantification of

cloudiness is often not objective. Indeed, only two states can be unequivocally defined: the completely cloudless sky and the overcast sky. Intermediate states will inevitably be approximate. The common approach to estimating the amount of clouds in retrospective calculations is to evaluate the ratio between the theoretical radiation at the top of the atmosphere, corrected for its calculated transparency, and the radiation measured at the nearest meteorological station [16]. Apparently, in this case the accuracy of defining of cloudiness will be higher. However, even this approach has drawbacks: intensification of the solar radiation flux by a cloud layer is widely known [24, 25].

It is obvious that in prognostic calculations such approach is impossible and it is necessary to implement one or another simplified scheme. Besides, it is not reasonable to link a parameterizing scheme either to peculiarities of a specific place (e.g., a mountain system or an area within such system) or to a specific type of clouds. In this study, we employed a simple scheme, which resembles to some extent an approach suggested in [17, 23]. This approach supposes linking cloudiness to daily precipitation amount. Implementation of this approach will obviously distort real instant data, nevertheless, averaging over long period, which is critically important for mass-balance calculations, allows obtaining results that are satisfactorily comparable with observations, as demonstrated below.

So, the total radiation in the presence of cloudiness is calculated similarly to the case of a cloudless atmosphere:

$$E_{\mathrm{S}}^{\mathrm{cl}} \quad nE_{\mathrm{dir}} \quad E_{\mathrm{dif}}^{\mathrm{cl}} \quad \widetilde{E}_{\mathrm{dif}}^{\mathrm{cl}} \tag{12}$$

where n is cloudiness from 0 to 1; E_{dir} is defined in (2); $E_{\mathrm{dif}}^{\mathrm{cl}}$ is radiation at single scattering in the cloudy atmosphere:

$$E_{\mathrm{dif}}^{\mathrm{cl}} \quad f_{\mathrm{S}}[T_{\mathrm{cl}} E_{\mathrm{dif}} \quad k^{*}(1 \quad T_{\mathrm{cl}})(E_{\mathrm{dir}} \quad E_{\mathrm{dif}})] \quad E_{\mathrm{t}}. \tag{13}$$

In (13) k^{*} is the empirical coefficient dependent on geographical latitude ($k^{*} = 0.33$ at 40 N [22]); T_{cl} is attenuation of the diffuse radiation by a cloud layer [14]:

$$T_{\mathrm{cl}} \quad 1 \quad n \quad n\exp(\ m_{\mathrm{R}}\,\mathrm{COD}) \tag{14}$$

where m_{R} is the atmospheric mass of the Rayleigh scattering (8); COD is cloud optical depth [13]. Formalization and evaluation of the latter parameter is rather complicated [13], that is why it is reasonable to consider it as a tunable one.

Similarly to (11), multiple scattering can be formulated as

$$\widetilde{E}_{\mathrm{dif}}^{\mathrm{cl}} \quad (E_{\mathrm{dir}}^{\mathrm{cl}} \quad E_{\mathrm{dif}}^{\mathrm{cl}})[\ _{\mathrm{g}} \ _{\mathrm{cs}}/(1 \quad _{\mathrm{g}} \ _{\mathrm{cs}})] \tag{15}$$

where $_{\mathrm{cs}}$ is albedo of the cloudy sky,

$$_{\mathrm{cs}} \quad _{\mathrm{R}} \quad _{\mathrm{a}} \quad _{\mathrm{c}} \tag{16}$$

where $_{\mathrm{c}} = 0.01653$ is albedo of clouds [22]; $_{\mathrm{R}}$ and $_{\mathrm{a}}$ are defined above; E_{t} is calculated similarly to (10) with replacement of the components taking into account cloudiness.

3. DATA

In order to compare simulation results with observations, we used in this study records of the automatic weather stations (AWS, Fig. 1) manufactured by Climantec Inc. (Japan) established on the glacier on the elevations of 3420 m (AWS1) and 3460 m (AWS2) above sea level. Global radiation on these AWS was measured by pyranometers CM3 manufactured by Kipp and Zonen (The Netherlands). Observations on the AWS1 started in July, 2017, on the AWS2, in August, 2018 and have been performed until present. Radiation has been measured with the 5-minute interval and was followed by hourly averaging. A small measurement interval with subsequent averaging allows avoiding sharp jumps in the measured radiation values, especially in the morning and evening hours, when the Sun is already (still) above the horizon, but the surrounding mountains obstruct direct radiation. In addition, short time interval allows more accurate capturing of times of the radiation maxima.

The nearest weather stations conducting observations of cloudiness, Kyzyl Suu and Tien Shan, are located approximately at the same distance (about 40 km) from the glacier. The Karabatkak glacier is separated from the AWS Kumtor by the Terskey Ala-Too mountain ridge, therefore, it is more reasonable to use the data from the Kyzyl Suu weather station. We analyzed a record of the regular observations for the time

Table 2. Mean annual cloudiness during the days with different amount of precipitation at the meteorological station Kyzyl Suu from October 1, 2016 to September 30, 2018 and the values used in the calculations

Period	No precipitation	Any precipitation	5 mm/day	>5 mm/day	>10 mm/day
Whole year	4.8	7.7	7.6	8.3	8.5
Control experiments					
Cold period	5.4	8.1	7.7	9.0	10.0
Warm period	4.2	7.5	7.5	7.7	7.7
Corrected values used in calculations					
Whole year	3.8	–	5.0	6.0	7.7

period from October 1, 2016 to September 30, 2018 (two hydrological years). This time segment has minimum number of gaps in the whole available record of 2005–2020 freely available at the site www.rp5.ru. Subsequently, the data were daily averaged and collated with the daily precipitation record for the same time period. Daily precipitation sums were measured using the Tretyakov pluviometer at the weather station of the Tien Shan High Mountain Scientific Center in Chon-Kyzyl Suu (Fig. 1). We considered data of the cold (October–March) and warm (April–September) periods separately. Besides, precipitation events were ranged according to the intensity (Table 2).

In the Table 2 "any precipitation" denote precipitation events, regardless of their amount. It is obvious that average cloudiness differs between the warm and the cold periods and slightly changes dependently on daily precipitation amount. Implementation of the simple scheme described above allowed linking cloudiness to the actual, and in the case of prognostic calculations, to the model generated precipitation amount [23].

Shading effect from the surrounding relief was evaluated in accordance with a widely used algorithm [10]. In overall, implementation of this algorithm yields realistic results, though the use of a smoothed digital elevation model leads to negligible distortions of the calculated radiation fluxes (discussed in Section 4). The same algorithm was used for calculation of the sky view factor f_s. The digital elevation model with the spatial resolution of 25 m was provided by the Water Problems and Hydropower Institute of the National Academy of Sciences of the Kyrgyz Republic.

4. RESULTS AND DISSCUSSION

To validate the correct operation of the radiation model, calculated values of the total radiation were compared with the AWS data. For more accurate comparison, the interval of calculations was the same as the interval of measurements. Local time was corrected using longitude of the glacier and solving the time equation [12].

Accurate comparison of the results for the particular dates has sense only in two cases: when it is possible to unequivocally determine that on that day the sky was cloudless (or, at least, in the time period of maximum insolation (Figs. 2a, 2c, and 2e) or overcast (Figs. 2b, 2d, and 2f). Note that the contribution to the global radiation of the calculated values of E_{dif}, which are often ignored in glaciological models, in a cloudless sky (11) and $E_{\text{dif}}^{\text{cl}}$ in an overcast sky (15) is 2–6% and 32–34%.

We must focus on some discrepancies between the observed and calculated global radiation data. Apparently, the overestimation of the calculated values in the morning hours happens because the spatial step in the employed digital elevation model is 25 m, which naturally leads to smoothing of the relief and the disappearance of some small-scale details that in reality create shading on the glacier surface. Besides, shading is calculated for the entire 25 25 m cell, and the automatic weather station is described as a point in the cell, which is also a source of uncertainty about entering or leaving the shadow area.

In the model, we use cloudiness averaged over eight daily standard measurements, therefore, increase of cloudiness between terms and, as a result, abrupt decrease of global solar radiation, cannot be reproduced by the model (Fig. 2c, 13:00–15:00). In the overcast case, direct radiation is absent, and the global radiation

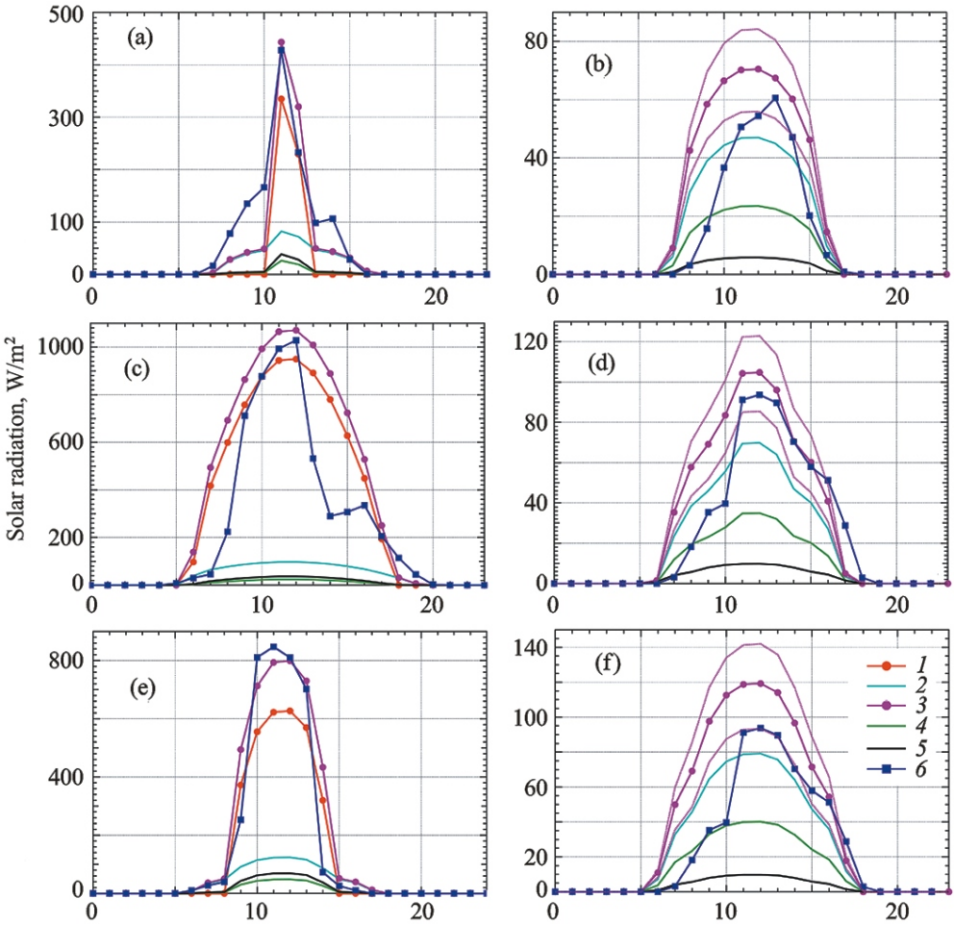

Fig. 2. Measured and modelled values of the global radiation and modelled components of the global radiation (a, c, e) in the clear sky conditions and (b, d, f) in the overcast conditions. (a) December 16, 2018; (b) January 16, 2018; (c) June 18, 2019; (d) February 19, 2020; (e) October 9, 2017; (f) March 7, 2020. Radiation fluxes: (*1*) is direct; (*2*) is diffuse; (*3*) is global; (*4*) is multiple reflected; (*5*) is reflected by the relief; (*6*) is measured global. The dot lines indicate maximum and minimum values of the modelled global radiation.

Table 3. Calculated values of the transmissivity coefficients t_a and t_w and the products ($_t$) of all in the true midday of 15th day of every month, their maximum (max $_t$) and minimum (min $_t$) values

Parameter	January	February	March	April	May	June	July	August	September	October	November	December
t_a	0.965	0.959	0.932	0.894	0.956	0.960	0.957	0.951	0.951	0.962	0.971	0.975
t_w	0.859	0.855	0.880	0.899	0.919	0.930	0.935	0.932	0.922	0.909	0.997	0.861
$_t$	0.725	0.753	0.748	0.730	0.786	0.788	0.782	0.772	0.762	0.755	0.738	0.724
max $_t$	0.736	0.796	0.783	0.756	0.802	0.801	0.796	0.791	0.781	0.770	0.749	0.731
min $_t$	0.718	0.740	0.718	0.708	0.772	0.778	0.769	0.755	0.746	0.742	0.731	0.720

$_t$ is the product of all coefficients at $t_R = 0.932$, $t_o = 0.979$, $t_n = 0.998$, $t_g = 0.988$.

consists of diffuse radiation only. Measured diffuse radiation is comparable with simulated figures taking into account its scatter in the limits of (is a root-mean-square error, see Table 1).

Total attenuation of the direct solar radiation in accordance with equation (2) depends on the solar zenith angle, as well as on the annual variability of the atmospheric pressure, turbidity factor, water vapor content, etc. Annual variability of those attenuating factors and the products of all factors are collected in Table 3.

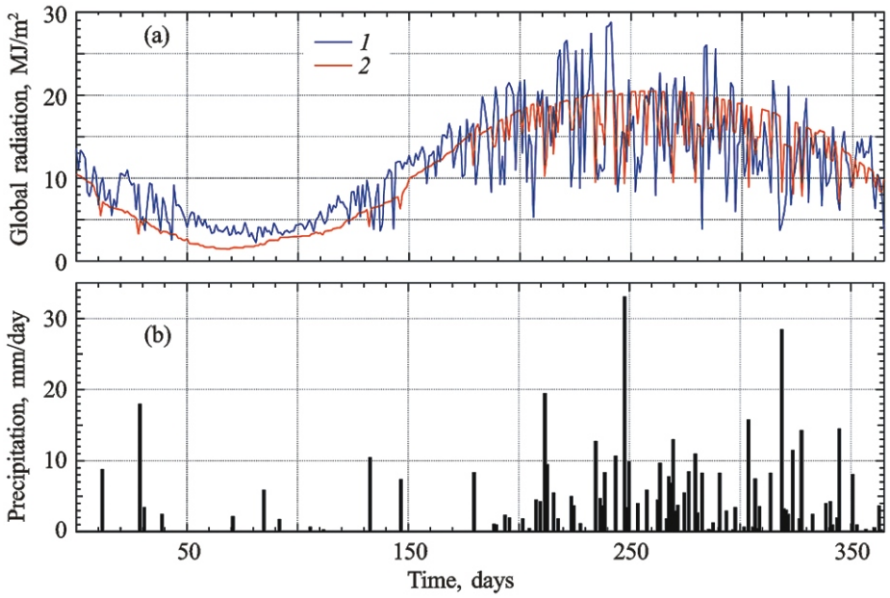

Fig. 3. (a; *1*) Measured and (*2*) modelled daily amount of the global radiation at the AWS1 in the hydrologic year from October 1, 2018 to September 30, 2019. (b) Daily amounts of precipitation at the Chon-Kyzyl Suu weather station during the same period.

Shown in the table, are maximum and minimum values, which were calculated form the sample root-mean-square errors (, , and $_w$). Resultant scatter of transmissivity does not apparently exceed 10%.

Precipitation events are mostly observed in the region in the second half of the year, from July to November. Maximum amplitudes of the global radiation also fall on this period (Figs. 3a and 3b). Note that the graph of the calculated radiation is smoothed, the peaks of the maximum values are cut off. It can be explained by employment of the fixed cloudiness. Since the number of the consecutive days without precipitation is greater than the days with precipitation, the cutoff from above occurs more often than from below. Minima in calculated radiation often exceed actual ones, because minimum cloudiness in the model is also limited.

In order to calculate melting rate in the model of surface mass balance, it is critically important to evaluate quantity of incoming solar radiation in the warm period of the year. Therefore, in this study comparison of the modelling results and the measurements is limited by the period from April to September (10-day period sums are shown in Fig. 4, and monthly ones, in Table 4). Measurements on the AWS1 were conducted during two warm periods in 2018 and 2019, on the AWS2, only during the year of 2019 (2020 data has not yet passed quality control).

The largest discrepancies between the model and actual amounts of radiation are observed in July–September with the maximum in August. Perhaps, this happens because during this period the real cloudiness deviates most from the average, which, accordingly, determines the difference between the simulation results and observations: the model overestimates radiation values. However, positive and negative deviations eventually compensate each other, smoothing the resulting deviations at the end of the ablation period, which ultimately matters for calculating total ablation.

After recalculation of the absolute difference between the modelled and measured radiation into the equivalent of the melted layer of ice and taking into account the conventional ice albedo of 0.3 and the specific heat of fusion of 334 kJ/kg, we obtain the upper estimate of the error in determining the ablation value in the current year. Since the balance of the longwave radiation, the layer of melted seasonal snow, albedo evolution, and other factors are not taken into account, we mean the upper boundary of the estimates. In 2018, in the altitudinal range of 3400–3500 m, the average surface melting determined from measurements on ablation stakes, was 3100 mm. Thus, on AWS1, the maximum error value for the entire ablation season was about 9%. A similar estimate for 2019 gives a value of about 13% for AWS1 and about 1% for AWS2.

Of course, linking amount of precipitation to the cloudiness will be limited to a specific geographical region. We assume that this is not a big problem. One way or another, a number of climatic and other regularities will determine the peculiarities of the dynamics of mountain glaciers. Within the framework of

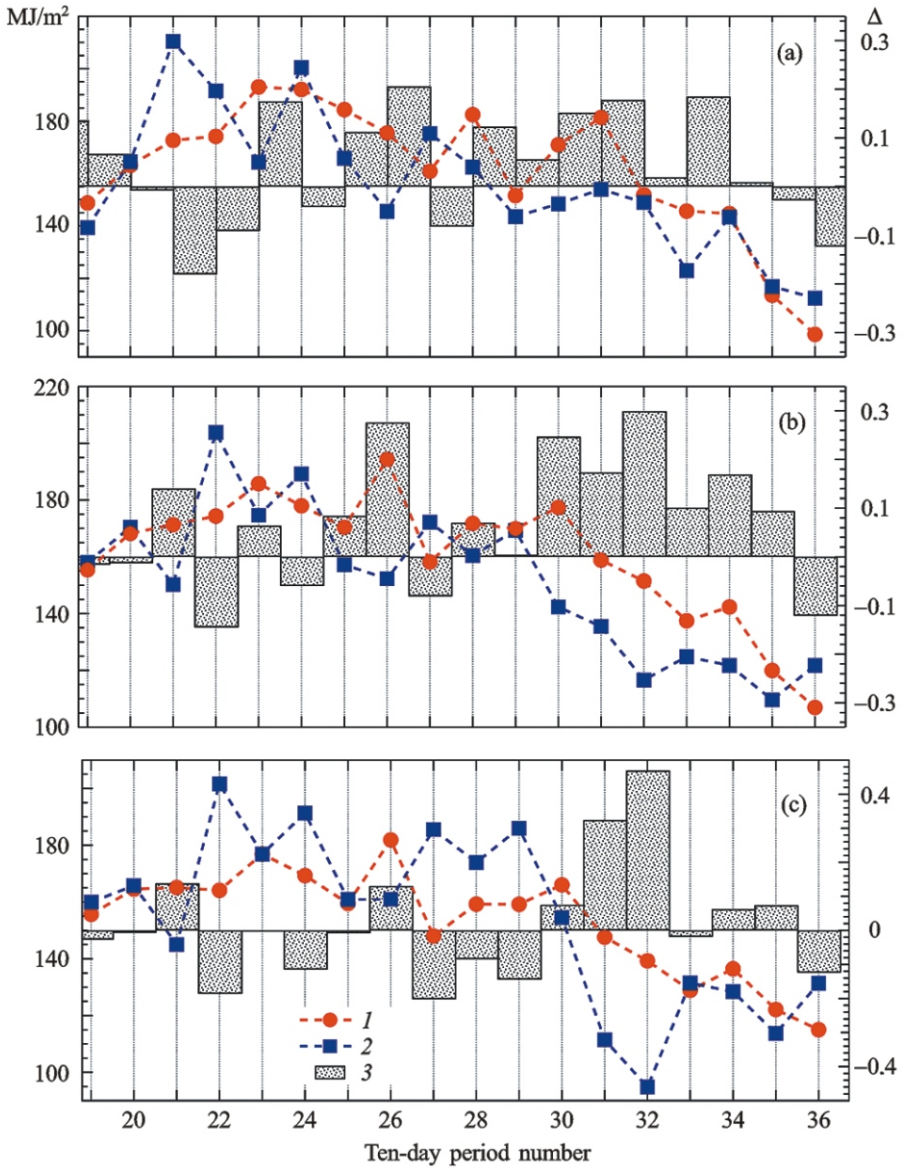

Fig. 4. (*1*) Modelled and (*2*) measured cumulative 10-day period amounts of global radiation (a) from April 1 to September 30, 2018 at the AWS1, from April 1 to September 30, 2019 (b) at the AWS1 and (c) AWS2 and (*3*) corresponding root-mean-square errors .

the unified approach, these peculiarities will determine the way of tuning the adjustable parameters of the mathematical model. Probably, it would be reasonable to calculate the attenuation of the radiation flux in the cloud layer based on the total water content in the clouds. Such an approach would of course be a rational solution if the purpose of the calculations were to determine the current melting rate on the surface of a mountain glacier, and data on the water content of clouds were available in one or another form. The purpose of this study was to elaborate a model focused on long-term prognostic calculations. From our point of view, we can hardly rely on the predictions of global or regional climatic modeling of cloudiness characteristics. The parameterization of cloudiness, as, in fact, the most powerful regulator of radiation fluxes, should be quite simple and base on quite obvious regional connections and relationships.

5. CONCLUSIONS

Correct calculation of the incoming shortwave radiation is critically important for elaboration of an energy balance model of the surface mass balance of mountain glaciers. Existing models often ignore, for example, multiple reflections between the Earth's surface or reflection from the surrounding terrain. When

Table 4. Modeled and observed (Obs.) values of the monthly amounts of global radiation (MJ/m^2), relative deviations of the model values from observed ones (Rel.) and equivalent of the difference between modelled and observed values in millimeters of the layer of the melted ice (Equ.)

Parameter	April	May	June	July	August	September	April–September
				AWS1, 2018			
Model	484.5	559.2	520.7	504.9	478.9	356.8	2904.0
Obs.	514.3	556.3	486.2	454.4	425.8	372.6	2809.0
Rel.	–5.8%	0.5%	7.1%	11.1%	12.5%	–4.2%	3.4%
Equ.	–89.2	8.7	103.3	151.2	159.0	–47.3	284.4
				AWS1, 2019			
Model	495.0	538.0	523.0	519.0	447.8	369.2	2892.1
Obs.	478.7	567.6	481.6	472.0	376.8	353.1	2729.9
Rel.	3.4%	–5.2%	8.6%	10.0%	18.8%	4.6%	5.9%
Equ.	34.2	–62.0	123.9	98.5	148.8	33.7	339.9
				AWS2, 2019			
Model	485.3	510.3	489.4	484.5	415.8	373.5	2758.9
Obs.	470.8	569.8	507.3	514.4	337.7	373.6	2773.5
Rel.	3.1%	–10.4%	–3.5%	–5.8%	23.1%	<–0.1%	–0.5%
Equ.	30.4	–124.7	–37.5	–62.7	163.7	–0.2	–30.6

clouds are absent or negligible, direct radiation dominates, and these processes are relatively insignificant. However, under overcast conditions, direct radiation is substantially weakened or even absent, and these sources play a significant role in the structure of diffuse radiation. It also seems to be a certain simplification to introduce a fixed ratio between direct and diffuse radiation. In calculations of atmospheric transmissivity, parameterization equations are often based on outdated or incomplete data on the composition of the atmosphere. All these reasons motivated us to critically revise computational algorithms in this study. We implemented algorithms developed earlier, which have never been used in glaciological applications. Parameterization of cloudiness is the most challenging task. Since prognostic calculations require simple schemes without excessive detailing concerning the type and layer of clouds, we relied on an obvious circumstance: on the day when precipitation falls, the cloudiness is on average higher than in the absence of the latter.

The results of simulations were compared with observations of the global radiation in 2017–2020 on two AMS installed on Karabatkak glacier. It was shown that the model with schematic cloud description satisfactorily reproduces observational data, including the warm half of the year, during the ablation season. Unfortunately, the limited scope of the paper did not allow us to include a comparison of the results obtained with reference multilinear calculations. We plan to do this in the future.

ACKNOWLEDGMENTS

The authors thank Muzapar Orozaliev for providing free access to the data of observations at Issyk Kul AERONET station and to the stuff members of the Tien Shan High Mountain Scientific Center, who sustain a system of meteorologic and glaciologic observations in the region.

FUNDING

The study was financially supported by the Russian Foundation for Basic Research, grant 20-05-000681 “Evolution of Glaciation of Inner Tien Shan under Climate Change and Technogenic Influence.” Solar radiation records were obtained under support of the Project 16H06291 of the Japan Society for the Promotion of Science (JSPS).

REFERENCES

1. K. Ya. Kondratiev, *Actinometry* (Gidrometeoizdat, Leningrad, 1965) [in Russian].
2. K. Ya. Kondratiev, Z. I. Pivovarova, and M. P. Fedorova, *Radiational Regime of Inclined Surfaces* (Gidrometeoizdat, Leningrad, 1978) [in Russian].
3. S. S. Kutuzov, "Change in Area and Volume of Glaciers of the Terskey Ala-Too Ridge in the Second Half of the 20th Century," Led i Sneg, No. 1, **52** (2012) [in Russian].
4. P. A. Morozova and O. O. Rybak, "Downscaling of the Global Climate Model Data for the Mass Balance Calculation of Mountain Glaciers," Led i Sneg, No. 4, **57** (2017) [in Russian].
5. E. P. Rets, N. L. Frolova, and V. V. Popovnin, "Modelling of Melting on the Surface of the Mountain Glacier," Led i Sneg, No. 4, **51** (2011) [in Russian].
6. O. O. Rybak, E. A. Rybak, N. A. Yaitskaya, et al., "Modeling the Evolution of Mountain Glaciers: A Case Study of Sary-Tor Glacier, Inner Tien Shan," Kriosfera Zemli, No. 3, **23** (2019) [in Russian].
7. N. S. Arnold, W. Gareth Rees, A. J. Hodson, and J. Kohler, "Topographic Controls on the Surface Energy Balance of a High Arctic Valley Glacier," J. Geophys. Res., **111** (2006).
8. J. L. Bamber and A. J. Payne, *Mass Balance of the Cryosphere: Observations and Modelling of Contemporary and Future Changes* (Cambridge University Press, Cambridge, 2004).
9. B. B. Chen, S. A. Imashev, L. G. Sverdlik, et al., "Ozone Variations over Central Tien Shan in Central Asia and Implications for Regional Emissions Reduction Strategies," Aerosol and Air Quality Res., **13** (2013).
10. J. Dozier and J. Frew, "Rapid Calculation of Terrain Parameters for Radiation Modeling from Digital Elevation Data," IEEE Trans. Geosci. and Remote Sens., **28** (1990).
11. C. A. Gueymard, "Direct Solar Transmittance and Irradiance Predictions with Broadband Models. Part I: Detailed Theoretical Performance Assessment," Solar Energy, **74** (2003).
12 . M. Iqbal, *An Introduction to Solar Radiation* (Academic Press, Toronto, 1983).
13. H. D. Kambezidis, B. E. Psiloglou, D. Karagiannis, et al., "Meteorological Radiation Model (MRM v6.1): Improvements in Diffuse Radiation Estimates and a New Approach for Implementation of Cloud Products," Renewable and Sustainable Energy Rev., **74** (2017).
14. H. D. Kambezidis, B. E. Psiloglou, D. Karagiannis, et al., "Recent Improvements of the Meteorological Radiation Model for Solar Irradiance Estimates under All-sky Conditions," Renewable Energy, **93** (2016).
15. D. G. Kaskaoutis and H. D. Kambezidis, "The Choice of the Most Appropriate Aerosol Model in a Radiative Transfer Code," Solar Energy, **82** (2008).
16. E. J. Klok and J. Oerlemans, "Model Study of the Spatial Distribution of the Energy and Mass Balance of Morteratschgletscher, Switzerland," J. Glaciol., No. 163, **48** (2002).
17. Y. Matsuda, K. Fujita, Y. Ageta, and A. Sakai, "Estimation of Atmospheric Transmissivity of Solar Radiation from Precipitation in the Himalaya and the Tibetan Plateau," Ann. Glaciol., **43** (2006).
18. J. Nemec, P. Huybrechts, O. Rybak, and J. Oerlemans, "Reconstruction of the Surface Mass Balance of Morteratschgletscher since 1865," Ann. Glaciol., **50** (2009).
19. S. Niemela, P. Raisanen, and H. Savijarvi, "Comparison of Surface Radiative Flux Parameterizations. Part II. Shortwave Radiation," Atmos. Res., **58** (2001).
20. F. Pellicciotti, B. W. Brock, U. Strasser, et al., "An Enhanced Temperature-index Glacier Melt Model Including Shortwave Radiation Balance: Development and Testing for Haut Glacier d'Arolla, Switzerland," J. Glaciol., **51** (2005).
21. F. Pellicciotti, T. Raschle, T. Huirlimann T., et al., "Transmission of Solar Radiation through Clouds on Melting Glaciers: A Comparison of Parameterizations and Their Impact on Melt Modelling," J. Glaciol., **57** (2011).
22. B. E. Psiloglou, M. Santamouris, and D. N. Asimakopoulos, "Atmospheric Broadband Model for Computation of Solar Radiation at the Earth's Surface. Application to Mediterranean Climate," Pure and Appl. Geophys., **157** (2000).
23. S. Ragettli, F. Pellicciotti, R. Bordoy, and W. W. Immerzeel, "Sources of Uncertainty in Modeling the Glaciohydrological Response of a Karakoram Watershed to Climate Change," Water Resour. Res., **49** (2013).
24. G. H. Yordanov, O.-M. Midtgard, T. O. Saetre, et al., "Overirradiance (Cloud Enhancement) Events at High Latitudes," IEEE J. Photovoltaics, **3** (2013).
25. J. Zhang, K. Watanabe, J. Yoshino, et al., "Physical Process and Statistical Properties of Solar Irradiance Enhancement Observed under Clouds," Japan. J. Appl. Phys., **57** (2018).